Inorganic Chemistry

Article

pubs.acs.org/IC

High-Temperature X-ray Diffraction Study of Uranium−Neptunium Mixed Oxides

Mélanie Chollet, Renaud C. Belin,* Jean-Christophe Richaud, Muriel Reynaud, and Frédéric Adenot

CEA, DEN, DEC, SPUA, LMPC, F-13108 Saint-Paul-lez Durance, France

ABSTRACT: Incorporating minor actinides (MAs = Am, Np, Cm) in UO_2 fertile blankets is a viable option to recycle them. Despite this applied interest, phase equilibria between uranium and MAs still need to be thoroughly investigated, especially at elevated temperatures. In particular, few reports on the U−Np−O system are available. In the present work, we provide for the first time in situ high-temperature X-ray diffraction results obtained during the oxidation of $(U_{1-y}Np_y)O_2$ uranium−neptunium mixed oxides up to 1373 K and discuss subsequent phase transformations. We show that (i) neptunium stabilizes the UO_2-type fluorite structure at high temperature and that (ii) the U_3O_8-type orthorhombic structure is observed in a wide range of compositions. We clearly demonstrate the incorporation of neptunium in this phase, which was a controversial question in previous studies up to now. We believe it is the particular stability of the tetravalent state of neptunium that is responsible for the observed phase relationships.

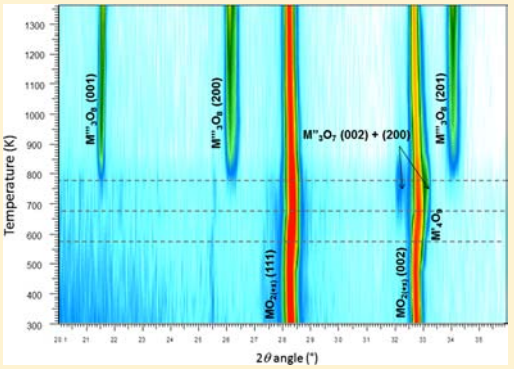

INTRODUCTION

Actinide oxides are an appealing research field not only for the obvious technological significance of these materials as nuclear fuels but also from a fundamental perspective, thanks to their various oxidation states and their capacity to deviate from stoichiometry.

In the framework of actinide recycling and transmutation in sodium fast neutron reactors, two options are considered: (a) homogeneously adding 2−6% of minor actinides (MAs) to the fuel (homogeneous mode) and (b) introducing MAs in higher amounts into fertile blankets (heterogeneous mode).[1] Indeed, regarding the second option, MAs bearing matrixes incorporating up to 20−30 wt % of MAs to be placed in specific assemblies in the periphery of the core are considered.

In this prospect, a better knowledge of phase relationships in U−MAs−O systems is of great interest for both the fabrication process and the behavior under irradiation. The present study focuses on neptunium bearing blankets because little is known about phase equilibria within the U−Np−O phase diagram, especially in the oxygen hyperstoichiometric domain (i.e., O/M > 2), and because such data are essential to improving the thermodynamic description of this system.

A substantial number of experimental studies on the oxidation mechanisms of UO_2 and associated kinetics are available,[2−6] and phase equilibria in the hyperstoichiometric domain are well described[7−9] at least up to 2000 K. Uranium has the ability to adopt high valence states (i.e., IV+, V+, and IV +) in the oxide solid form, which involves several hyperstoichiometric products. First, when subjected to an oxidizing thermal treatment, the stoichiometric fluorite-type phase UO_2 accommodates oxygen atoms as interstitial defects to form the UO_{2+x} compound, with x the oxygen hyperstoichiometry factor. The maximum oxygen incorporation is temperature-dependent. For example, within the range 400−500 K, x does not exceed the value of 0.03[2], whereas at 1500 K, the composition can reach $UO_{2.25}$. At low temperatures and for higher values of x, the additional oxygen atoms are accommodated in a fluorite superstructure, i.e., U_4O_{9-y}, thereby forming a UO_{2+x}−U_4O_{9-y} biphasic region. The latter phase is known to oxidize from U_4O_{9-y} to the stoichiometric composition U_4O_9. A metastable tetragonal phase, whose composition is U_3O_7, is observed up to ca. 650 K. For O/U between 2.25 and 2.6, the orthorhombic structure U_3O_8 forms and coexists with UO_{2+x} above 1400 K and with U_4O_9 below. Similarly to U_4O_9, U_3O_8 is not a stoichiometric compound and its monophasic domain extends from O/U = 2.6 to the limit value of $^8/_3$.

Unlike uranium, little is known on neptunium in the oxide form. Occupying an intermediate position between uranium and plutonium in the actinide series, neptunium has a strong propensity to remain tetravalent in solid-state compounds, as in the dioxide NpO_2, which is very stable regardless of the atmosphere.[10] As opposed to UO_2, the NpO_2 fluorite-type phase has no hyperstoichiometric domain of existence. The only reported phase for O/Np > 2 is the monoclinic phase Np_2O_5, whose domain is very limited and poorly defined.[11] Unsuccessful efforts were made to prepare Np_2O_5 via oxidation of NpO_2, with the phase being highly unstable and readily decomposing to $2NpO_2 + {}^1/_2O_2$.[10]

Regarding the $(U_{1-y}Np_y)O_{2+x}$ system, very few experimental studies are available. Paul and co-workers[12,13] studied the quasi-binary UO_{2+x}−NpO_2 phase diagram in O_2 between 1373 and 1823 K and reported three regions: a narrow U_3O_8 phase at the uranium-rich side with a partial substitution of uranium by

Received: November 9, 2012
Published: February 14, 2013

   dx.doi.org/10.1021/ic302457m | *Inorg. Chem.* 2013, 52, 2519−2525

neptunium; a two-phase region composed of U_3O_8 and of a fluorite solid solution (MO_{2+x}; M = U + Np); a wide MO_{2+x} solid solution at the neptunium-rich side for $y > 0.55$. Alain[14] described a linear evolution between the lattice parameter and the composition of the MO_{2+x} phase at 1273 K in vacuum. Yamashita et al.[15] carried out a high-temperature X-ray diffraction (XRD) study on $(U_{1-y}Np_y)O_{2+x}$ samples in He−8% H_2, CO_2−1% CO, N_2−100 ppm O_2, N_2−1% O_2, and air but report phase equilibria at 1273 K only. Like Paul's observations, this work highlights the formation of a biphasic domain, U_3O_8 + $(U_{1-y}Np_y)O_{2+x}$, when stoichiometric materials are heated under an oxidizing atmosphere from $y = 0.2$ to 0.65. For $y > 0.65$, the hyperstoichiometric $(U_{1-y}Np_y)O_{2+x}$ material is monophasic. However, both studies diverge regarding neptunium solubility in the U_3O_8 phase. From chemical analysis, Paul observed a slight incorporation of neptunium, whereas Yamashita et al. assumed the absence of neptunium in the U_3O_8 phase. However, Finch and Kropf[16] later reported the synthesis of a $(U_{1-y}Np_y)_3O_8$ monophasic material without evidencing residual NpO_2, which tends to demonstrate the miscibility of neptunium within the orthorhombic structure. To our knowledge, no other data are available regarding phase equilibria and oxidation processes in the hyperstoichiometric domain of the $(U_{1-y}Np_y)O_{2+x}$ system.

To go further, the comparison with both uranium−lanthanides (Ln) and uranium−plutonium mixed oxides under oxidizing conditions is interesting. Uranium−Ln mixed oxide systems have been extensively studied[17−19] because Ln cations are often considered as good surrogates of actinides because of their comparable atomic radii. They remain predominantly trivalent in oxide solid-state compounds, with cerium being, however, both trivalent and tetravalent. The U−Pu−O system was investigated[20−23] because of its significance in the frame of current nuclear fuels. It is comparable with the U−Np−O system because plutonium does not have higher valence states than IV+ in oxide solid-state compounds.

In the present study, we performed for the first time in situ high-temperature XRD experiments on $(U_{1-y}Np_y)O_2$ samples in air, from room temperature up to 1373 K with 100 K increments on $y = 0.1$, 0.3, and 0.7 compounds as well as on pure UO_2 and NpO_2. Our results are compared to those available in the literature for U−Pu−O and similar systems in the Ln series, with particular attention on the domain of existence of the fluorite MO_{2+x} structure and its concomitant occurrence with the orthorhombic M_3O_8 structure. Regarding the U−Np−O system, we confront our data to those previously reported and focus on both similarities and discrepancies with a special emphasis on the occurrence of the orthorhombic U_3O_8 phase and on its ability to incorporate neptunium.

MATERIALS AND METHODS

Three stoichiometric powder samples of $(U_{1-y}Np_y)O_2$, $y = 0.1$, 0.3, and 0.7, were prepared starting from UO_2 and NpO_2 ground and mixed in the appropriate ratios and calcined under a reducing atmosphere (i.e., Ar/5% H_2) at 1773 K for 2 × 20 h with an intermediate grinding.

Room-temperature and in situ high-temperature XRD measurements were performed with a Bragg−Brentano θ−θ Bruker D8 Advance X-ray diffractometer combined with a heating stage and implemented in a glovebox dedicated to nuclear material handling at the LEFCA facility (CEA Cadarache, France). Experiments were carried out starting from pure UO_2 and NpO_2 as well as from the stoichiometric mixed oxides. The X-ray beam was supplied by a conventional Cu radiation tube source ($K\alpha_1$ + $K\alpha_2$ radiation, λ = 1.5406 and 1.5444 Å) used at 40 kV and 40 mA. A Ni foil filtered the $K\beta$ radiation. The signal was detected by a LynX'Eye fast-counting PSD detector with an opening angle of $2\theta = 3°$. A MRI Physikalische Gerate GmbH TC-Radiation heating stage was used with a platinum strip as a direct heater and a platinum radiant heater suited for oxidizing conditions.

Preceding any setup adjustments, a temperature calibration was carried out in steps of 100 K over the temperature range of interest, 293−1500 K using MgO. MgO lattice parameters as a function of the temperature were taken from previously reported values.[24] Taking into account the propagation of errors on the lattice parameter measurements and the slight discrepancies in reproducibility, uncertainties on the temperature are estimated to be ±15 K whatever the temperature.

About 20 mg of powder was spread in a thin layer on the heating strip. Prior to each set of measurements, a rocking curve and displacement corrections were systematically applied to take into account the strip angular position and displacement. Then, the specimen stage was purged with high-purity helium followed by a vacuum of 10^{-5} mbar.

Diffraction patterns were acquired over a 2θ interval from 20° to 145° by steps of 0.02° during 0.3 s, leading to a complete pattern acquisition in ca. 20 min. A series of XRD patterns were collected isothermally in air from room temperature to 1373 K with 100 K steps and with a rate of 5 K/s between each pattern acquisition. One pattern was recorded at room temperature after slow cooling of 4.4 K/min.

Patterns were analyzed using the *TOPAS v.4* software package[25] according to the Pawley method[26] and based on the fundamental parameter approach that adequately fits the instrumental contributions to the observed peak profiles (geometry, tube type, and slit system).[27]

The line profile shapes are described by convoluting the wavelength distribution of the emission profile, considering the instrument geometry, aberrations, and physical properties of the sample. The microstructural contributions were simulated with a physical broadening function added to the refinement. The background was approximated by a Chebyshev polynomial function with three terms. The refinement procedure considers first the zero detector and background parameters and then the lattice parameter and crystallite size. Refinements were obtained with Rwp factors ranging from 6 to 10, and the final error on the lattice parameter value ranges from 10^{-3} to 1×10^{-2} Å, depending of the amount of the phase in the sample.

RESULTS

Stoichiometric Materials. The monophasic nature of the stoichiometric $(U_{1-y}Np_y)O_2$ samples at room temperature was evidenced both by the sharp lines of the X-ray patterns indicating a solid solution and by the absence of residual dioxides (Figure 1a). All lattice parameters are in nice agreement with Vegard's law between stoichiometric UO_2 and NpO_2 end members, confirming the stoichiometry of the synthesized compounds (Figure 1b).

Evolution of the NpO_2 Lattice Parameter with temperature. As expected, according to the stability of the tetravalent state of neptunium in the oxide form, no phase transition or departure from stoichiometry is observed for NpO_2. The lattice parameter varies linearly from room temperature up to 1377 K in air (Figure 2). Thermal expansion is in nice agreement with the previous data of Yamashita et al.[28] obtained in He/8% H_2 and in air, demonstrating that NpO_2 remains stoichiometric. These data allow calculation of the thermal expansion coefficients (tec). Lattice parameters were fitted using a second-order polynomial, and the resulting tec values are 8.4×10^{-6} K^{-1} at 300 K and 10.9×10^{-6} K^{-1} at 1200 K. They are very close to those of Yamashita et al. (8.8×10^{-6} K^{-1} at 300 K and 10.8×10^{-6} K^{-1} at 1200 K).

Hyperstoichiometric Materials. Figures 3 and 4 show isodensity maps of XRD patterns recorded during the whole experiment from 20 to 37−50° 2θ for the UO_2 sample and at y

dx.doi.org/10.1021/ic302457m | Inorg. Chem. 2013, 52, 2519−2525

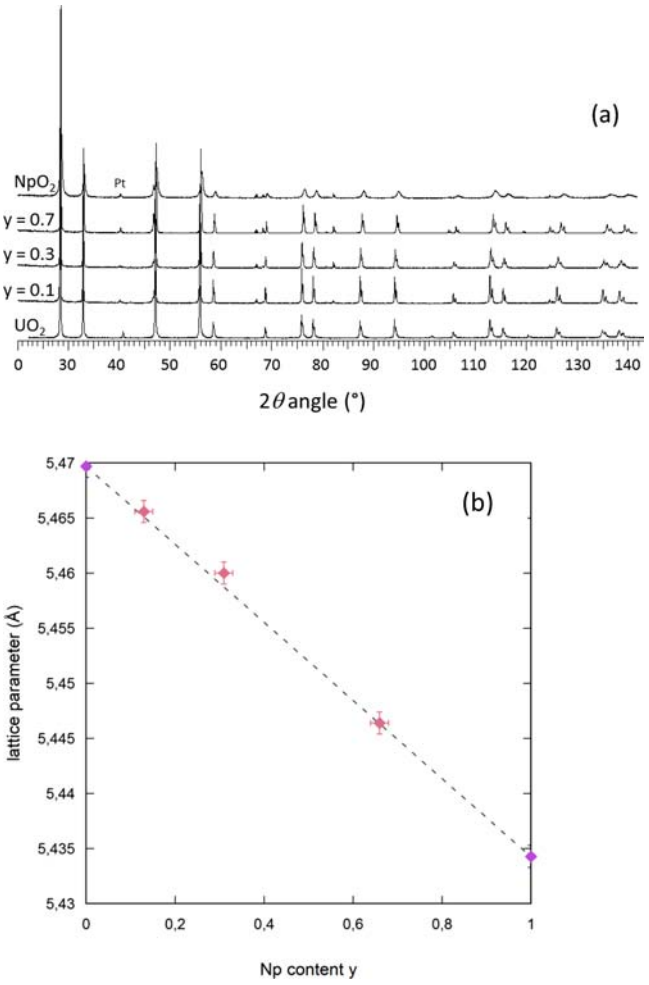

Figure 1. (a) XRD patterns of the initial $(U_{1-y}Np_y)O_2$ stoichiometric samples with y = 0.1, 0.3, and 0.7 compared to pure UO_2 and NpO_2. (b) Lattice parameters of $(U_{1-y}Np_y)O_2$ stoichiometric samples as a function of the composition following Vegard's law between UO_2 and NpO_2 end members.

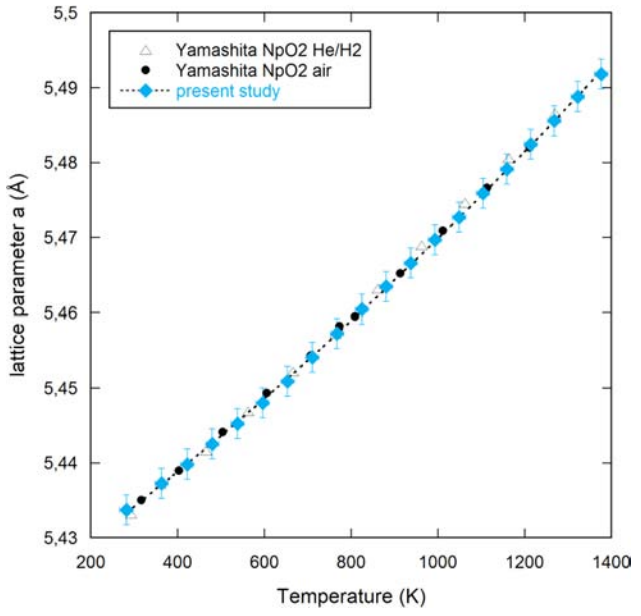

Figure 2. Evolution of the NpO_2 lattice parameter as a function of the temperature in air compared to Yamashita et al. in He/8% H_2 and in air.[28]

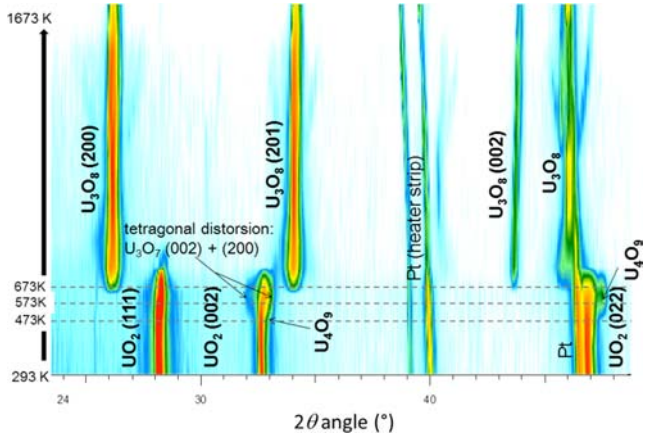

Figure 3. Isodensity map of the XRD peak intensity of the UO_2 sample in air from 24° to 50° as a function of the temperature.

= 0.1, 0.3, and 0.7, respectively, in air. This restricted angular range allows the main peaks of all phases considered in the study to be distinguished and different oxidation steps to be depicted. On a general basis, newly formed phases exhibit broad reflections, as was widely reported in U−O oxidation studies.[2,3,5] This broadening is interpreted as the sum of various contributions: small crystallite size, strain induced by crystallization, and a wide range of composition and stoichiometry.

In situ XRD measurements on UO_2 from room temperature to 1673 K are shown in Figure 3. The oxidation sequence is in good agreement with that previously reported,[5] that is

$$\begin{aligned} UO_2 &\xrightarrow{473\ K} UO_{2+x} + U_4O_9 \\ &\xrightarrow{573\ K} UO_{2+x} + U_4O_9 + U_3O_7 \\ &\xrightarrow{673\ K} U_4O_9 + U_3O_7 + U_3O_8 \\ &\xrightarrow{773\ K} U_3O_8 \end{aligned}$$

$(U_{1-y}Np_y)O_{2(+x)}$ mixed oxide compositions, y = 0.1, 0.3, and 0.7, show both similitudes and discrepancies upon oxidation in air (Figures 4 and 5).

From 300 to 573 K, the fluorite-type face-centered-cubic (fcc) stoichiometric solid solution phase MO_2 (space group 225 $Fm\bar{3}m$), with M = U + Np, expands with temperature for all compositions. At 573 K, diffraction peaks suddenly shift toward high angles, which corresponds to a decrease in the lattice parameters. This accounts for oxidation of the compound into a MO_{2+x} phase. This is also clearly visible on the evolution of the $MO_{2(+x)}$ phase lattice parameters as a function of the temperature (Figure 5a). At y = 0.3 and 0.7, lattice parameters of the MO_{2+x} phase are nearly identical at all temperatures above 573 K (Figure 5a). Their evolution is linear and, although higher, parallel to stoichiometric NpO_2. At y = 0.1, the evolution is not as straightforward as it crosses the NpO_2 line at 1073 K. Because the composition may be richer in uranium, it is probably more oxidized than the y = 0.3 and 0.7 compositions.

Meanwhile, at 573 K, at y = 0.1 and 0.3, the occurrence of shoulders in all of the reflection lines at high angles indicates the formation of a second fcc phase that we attribute to a

dx.doi.org/10.1021/ic302457m | Inorg. Chem. 2013, 52, 2519−2525

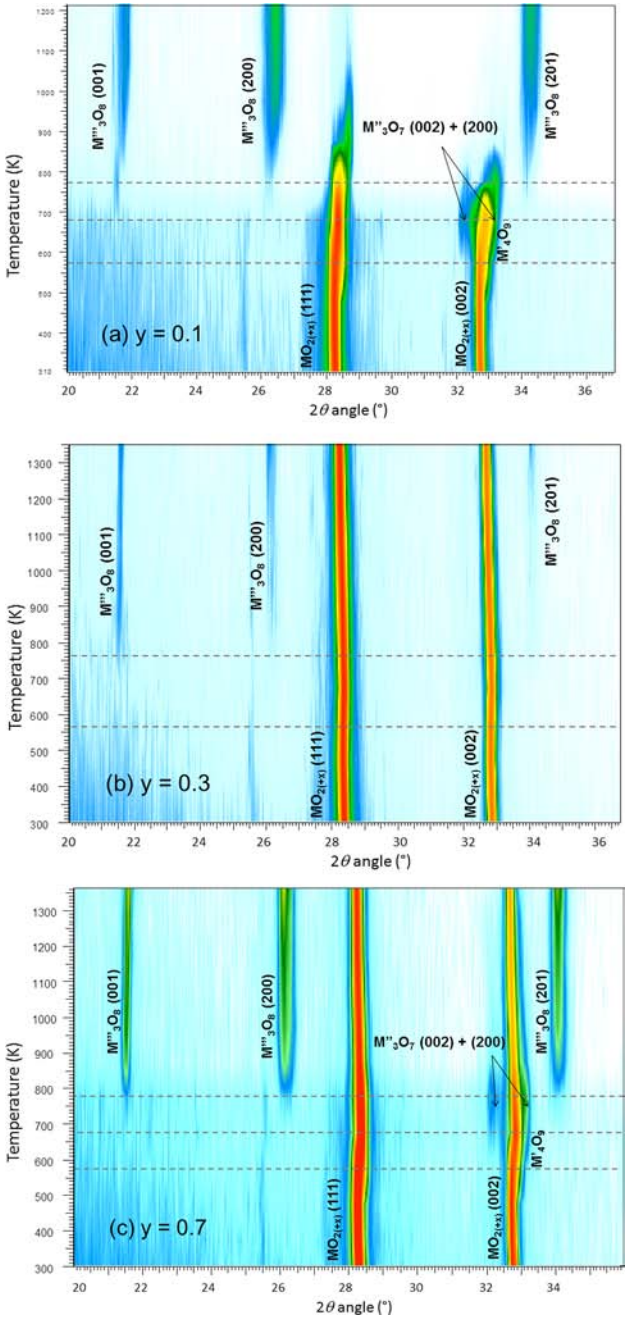

Figure 4. Isodensity maps of the XRD peak intensities of y = (a) 0.1, (b) 0.3, and (c) 0.7 samples in air from 21° to 37° 2θ as a function of the temperature.

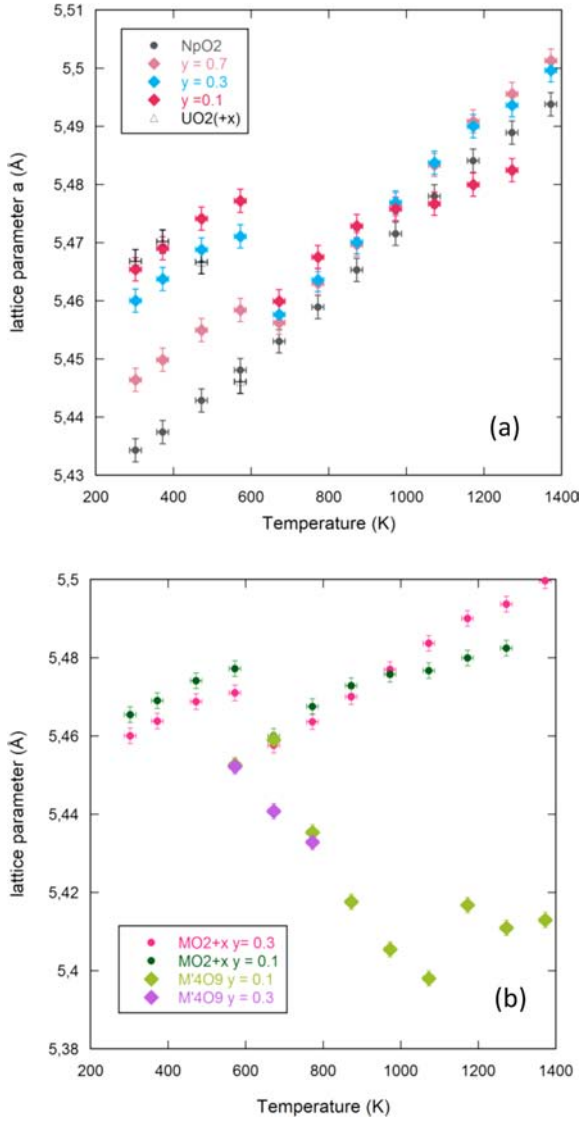

Figure 5. (a). Evolution of the $MO_{2(+x)}$ lattice parameter as a function of the temperature at y = 0, 0.1, 0.3, 0.7, and 1 in air. (b) Evolution of $MO_{2(+x)}$ and M'_4O_9 lattice parameters at y = 0.1 and y = 0.3 as a function of the temperature. Lattice parameters of the M'_4O_9 phases are divided by 4 for clarity.

M'_4O_{9-z} superstructure type phase (space group 214 $I4_132$) according to the oxidation sequence of UO_2, although no supplementary superlattice peaks related to this phase could be detected on the patterns (see Figure 6a,b). At y = 1, the lattice parameter of M'_4O_{9-z} progressively decreases from 4 × 5.459(2) to 4 × 5.398(2) Å as the temperature increases from 773 to 1073 K (Figure 5b). This decrease reflects the progressive oxidation of nonstoichiometric M'_4O_{9-z} to M'_4O_9. Then, it expands up to 4 × 5.413(2) Å at 1373 K, prior to disappearance of the phase. At y = 0.3, M_4O_{9-z} disappears at 773 K (Figures 4 and 5b).

At 673 K, at y = 0.1 and 0.3, two reflections appear on both sides of the (002) line of the MO_{2+x} phase. They reflect a tetragonal distortion into (200) and (002) reflections.[5] By analogy with the oxidation sequence occurring in the U−O system, this tetragonal phase will be named M''_3O_7 (space group 107 $I4mm$) in the following because its O/M composition is probably comparable. This metastable phase is only present over 100 K and disappears above 773 K. In the U−O system, the ratio of lattice parameters c/a of the U_3O_7 β-form phase is often discussed.[2,4,5] This value progressively reaches 1.031 during oxidation and then does not vary with the temperature or oxygen composition above 523 K. However, intermediate values between α-U_3O_7 (c/a = 0.989) and β-U_3O_7 were observed in nonisothermal studies. The value we obtained for M''_3O_7 at y = 0.3 is 1.021(2) at 673 K. It indicates that the oxidation in M''_3O_7 is incomplete, most likely because thermodynamic equilibrium is not achieved in the present experiment. This statement assumes that neptunium incorporation should not have any effect on the c/a ratio, by analogy with plutonium. Indeed, Benedict and Sari[29] do not observe

dx.doi.org/10.1021/ic302457m | Inorg. Chem. 2013, 52, 2519−2525

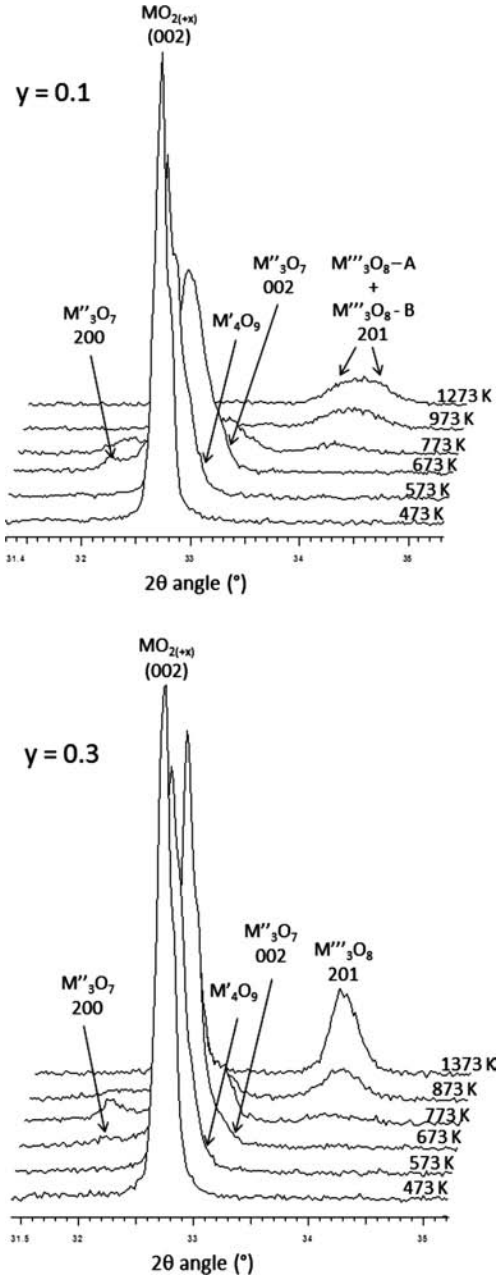

Figure 6. Selected XRD patterns for y = (a) 0.1 and (b) 0.3 over the range 31−35° 2θ.

noticeable changes in the lattice parameters with plutonium incorporation in U_3O_7 as high as y = 0.2.

No intermediate phases M'_4O_9 or M''_3O_7 are observed for the high neptunium total content sample y = 0.7.

Finally, at 773 K, the orthorhombic M'''_3O_8 (space group 38 *C*2*mm*) appears for all compositions and coexists with the remaining MO_{2+x} phase. As opposed to previous studies,[15] the occurrence of the M'''_3O_8 phase is observed for the first time up to y = 0.7. At y = 0.1, phase separation into two orthorhombic phases arises (Figure 6a). Lattice parameters at room temperature are reported in Table 1 and will be discussed later.

DISCUSSION

Comparison with the U−O System. The sequence of formation of oxidized phases M'_4O_9, M''_3O_7, and M'''_3O_8 in the U−Np−O system is similar to that of the U−O system.

Table 1. Lattice Parameters of the Orthorhombic M'''_3O_8 Phases at Room Temperature after Cooling for Both M'''_3O_8 at y = 0.1, 0.3, and 0.7[a]

		lattice parameters (Å)		
		a	*b*	*c*
U_3O_8		6.716(1)	11.960(1)	4.147(1)
M'''_3O_8	y = 0.1 − *A*	6.725(4)	11.930(4)	4.141(4)
	y = 0.1 − *B*	6.758(4)	11.882(4)	4.102(4)
	y = 0.3	6.756(4)	11.869(2)	4.152(4)
	y = 0.7	6.73(1)	11.96(1)	4.15(1)

[a]Lattice parameters of pure U_3O_8 are also indicated for comparison.[8]

However, the presence of neptunium induces some differences. First, in the U−Np−O system, all phase transformations occur 100 K higher than in UO_2. More surprisingly, while the MO_{2+x} fluorite phase disappears at 673 K in the U−O system, it coexists with M'''_3O_8 from this temperature up to the highest reached during our experiment. Therefore, the fluorite structure under oxidizing conditions is stabilized with the addition of neptunium. As opposed to the U−O system, where the highest oxidation states of uranium (V+ and VI+) allow complete oxidation of UO_2 in U_3O_8, no monophasic domain M'''_3O_8 is evidenced in the case of U−Np−O. Indeed, neptunium remains tetravalent even under oxidizing conditions (Figure 2) and is accommodated in the MO_{2+x} phase. In M'_4O_9, M''_3O_7, and M'''_3O_8 phases, O/M ranges from 2.25 to 2.67, which excludes the complete incorporation of tetravalent neptunium in such structures. In summary, the oxidation of $(U_{1-y}Np_y)O_2$ compounds is between that of pure NpO_2 and UO_2, that is, on the one hand, the persistence of the fluorite structure accommodating tetravalent cations and, on the other hand, the formation of phases with higher O/M and higher valence cations.

Neptunium Content in the MO_{2+x} and M'''_3O_8 Phases. Because neptunium and uranium cations have a conflicting behavior, adopting different valence states, a segregation Np/U is induced in the MO_{2+x} and M'''_3O_8 phases.

Figure 7 presents the lattice parameters *a*, *b*, and *c* of the orthorhombic M'''_3O_8 phases at room temperature after cooling for the three compositions y = 0.1, 0.3, and 0.7 normalized to those of pure U_3O_8[8]. These lattice parameters show a strong disparity versus the neptunium content.

At y = 0.1 and 0.3, they differ from that of pure U_3O_8. At y = 0.3, *a* is larger while *b* is smaller and *c* is identical. At y = 0.1, where a separation into two M'''_3O_8 phases occurs, one is quite similar to U_3O_8, whereas the other has lattice parameters closer to those observed at y = 0.3. The solubility of neptunium in the U_3O_8 phase has already been experimentally studied by Finch and Kropf.[16] They synthesized fully monophasic stoichiometric $(U_{1-y}Np_y)_3O_8$ samples with various neptunium contents from a liquid route and characterized them with XRD at room temperature. They observed a deviation from the lattice parameters of U_3O_8 similar to that evidenced at y = 0.3 in our study. They also quantified neptunium content as a function of each lattice parameter. Assuming that the oxygen stoichiometry in the M'''_3O_8 phases is known, we used these expressions at y = 0.1 and 0.3 and obtained a neptunium content close to 0.1 for both compositions. Consequently, taking into account the uncertainties, both M'''_3O_8 phases may have the same composition, which most likely indicates that the limit of incorporation of neptunium in U_3O_8 is of 10%, although a neptunium-free phase occurs at y = 0.1. This result

dx.doi.org/10.1021/ic302457m | *Inorg. Chem.* 2013, 52, 2519−2525

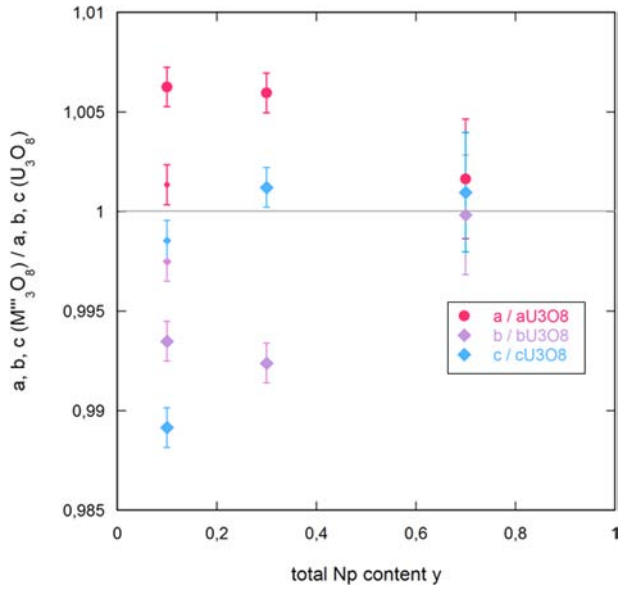

Figure 7. Lattice parameters *a*, *b*, and *c* of the M'''_3O_8 phases at $y = 0.1$ (two phases), 0.3, and 0.7 normalized to those of pure U_3O_8[8].

contradicts that of Finch and Kropf, who, using a different synthesis route, report a solid solution from U_3O_8 to $(U_{0.66}Np_{0.33})_3O_8$.

At $y = 0.7$, reflection lines of the M'''_3O_8 phase are broad and very weak compared to those of MO_{2+x}. Taking into account the uncertainties, the lattice parameters of M'''_3O_8 are close to those of U_3O_8, but neptunium incorporation in the structure is not to be excluded. Assuming that the oxygen stoichiometry is constant and because the M'''_3O_8 phase is in small amounts, it is therefore obvious that most of the neptunium is incorporated within the concurrent fcc structure, i.e., with a composition close to $(U_{0.3}Np_{0.7})O_{2+x}$.

Figure 8 shows the lattice parameter of the MO_{2+x} phases at selected temperatures as a function of the neptunium content.

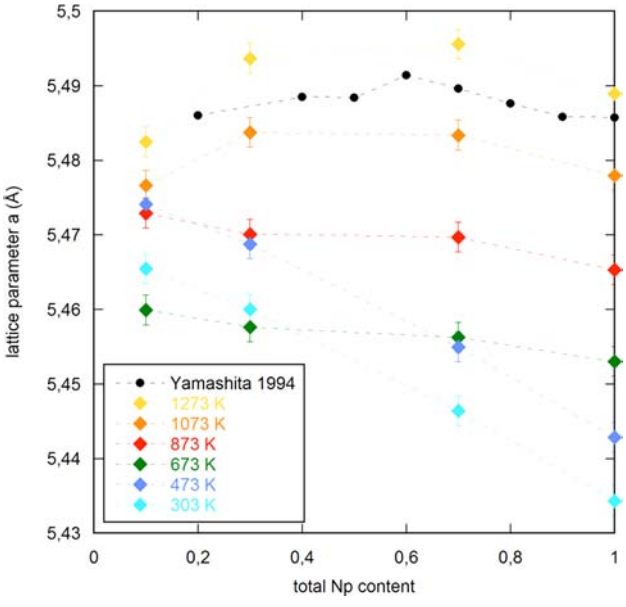

Figure 8. Lattice parameters of $MO_{2(+x)}$ and NpO_2 as a function of the total neptunium content in the samples at selected temperatures compared to those of Yamashita et al.[15] available at 1273 K.

Up to 473 K, when no phase transition has yet occurred, the lattice parameter roughly follows Vegard's law. Above 473 K, it becomes nearly independent of the neptunium content. Especially at $y = 0.3$ and 0.7, its value is identical up to 1273 K, therefore demonstrating that the neptunium content is the same and corresponds to the stoichiometry $(U_{0.3}Np_{0.7})O_{2+x}$, as mentioned earlier. This stands for the confirmation of a Np/U segregation with the emergence of a neptunium-enriched MO_{2+x} phase and a neptunium-depleted M''_3O_8 phase. Unfortunately, the determination of the MO_{2+x}/M'''_3O_8 ratio with the Rietveld method was not accurate enough, with the signal-to-noise ratio being too low and reflections too broad. Thus, a complete mass balance was not achievable, and it was difficult to go further into this discussion.

The Yamashita et al. study,[15] performed at 1273 K only, evidences a slightly smaller MO_{2+x} lattice parameter than that in the present study at the same temperature, although no uncertainties are given. Their compounds may be more oxidized because of 6 h of annealing compared to the 20 min used in this study. The values obtained by Yamashita et al.[15] do not follow Vegard's law, also indicating a Np/U segregation between MO_{2+x} and M_3O_8. Thus, contrary to the authors' assumption, some neptunium incorporation in the U_3O_8 phase is possible.

Comparison with the U−Pu−O and U−Ce−O Systems. Oxidation studies of $(U_{1-y}Pu_y)O_2$ solid solutions were mainly performed by quenching samples from various temperatures under controlled oxidizing atmospheres, followed by XRD characterization at room temperature.[20−23,30] The coexistence of MO_{2+x} with a second fcc structure, interpreted as M_4O_9, is observed for $2.20 < O/M < 2.27$ and a plutonium content up to $y = 0.3$. A metastable M_3O_7-type phase replaces MO_{2+x} for higher O/M up to $y = 0.25$ but is not present after 20 h of annealing. These studies are consistent with the intermediate phases M'_4O_9 and M''_3O_7 that we evidenced at $y = 0.1$ and 0.3 only in the U−Np−O system.

In the U−Pu−O system, monophasic $(U,Pu)_3O_8$ is observed only for $y < 0.1$, and for the highest O/M, a biphasic domain composed of fcc and M_3O_8-type phases is observed for $0.1 < y < 0.5$. In the U−Np−O system, this biphasic domain extends up to $y = 0.7$. The incorporation of plutonium in U_3O_8 was quantified during oxidation in air of $(U,Pu)O_2$ compounds using the b/a ratio.[21,24−26,30] Reported incorporation values are 0.1 at 1023 K,[30] 0.06 at 1273 K up to $y = 0.4$,[31] and 0.1 for $y = 0.2$.[23] Those values compare well with the maximum neptunium content of 10% that we have evaluated for M'''_3O_8.

The present results match also the oxidation studies of $(U_{1-y}Ce_y)O_2$ compounds, which evidence a large domain of stability of a hyperstoichiometric MO_{2+x}-type phase. At $y < 0.4−0.5$, a concomitant M_3O_8 phase is observed. Cerium is also the only Ln whose solubility was observed in the U_3O_8 phase at a limit content of 10%.[32]

CONCLUSION

In the present work, we performed in situ oxidation experiments on $(U_{1-y}Np_y)O_2$ compounds up to 1373 K in air for the first time. We evidenced various oxidation steps depending on the temperature and neptunium content. At $y = 0.1$ and 0.3, the sequence of oxidation is

dx.doi.org/10.1021/ic302457m | Inorg. Chem. 2013, 52, 2519−2525

$$MO_2 \xrightarrow{573\ K} MO_{2+x} + M'_4O_{9-z}$$
$$\xrightarrow{673\ K} MO_{2+x} + M'_4O_{9-z} + M''_3O_7$$
$$\xrightarrow{773\ K} MO_{2+x} + M'''_3O_8(\pm M'_4O_{9-z})$$

and at $y = 0.7$, it is

$$MO_2 \xrightarrow{573\ K} MO_{2+x} \xrightarrow{773\ K} MO_{2+x} + M'''_3O_8$$

Although it shows similarities with that observed for UO_2, the stability of tetravalent neptunium induces significant discrepancies. The fcc MO_{2+x} phase is stabilized up to 1373 K and coexists with the M'''_3O_8 phase. The neptunium content in the MO_{2+x} phase is close to 70%, regardless of the y value. In the U−O system, only monophasic U_3O_8 is present at high temperature because of the ability of uranium to adopt higher valence states (V+ and VI+). The occurrence of the M'''_3O_8 phase up to $y = 0.7$ was never observed in previous studies on U−Np−O or analogous systems involving both uranium and a tetravalent cation. We also demonstrate the incorporation of neptunium into this phase up to 10%, contradicting Yamashita's assumption that no neptunium is accommodated in U_3O_8.

We believe this original study provides fundamental data that are useful to improve the understanding of the U−Np−O system.

To complement the present work, X-ray absorption spectroscopy experiments performed on the same hyperstoichiometric samples are ongoing. Through probing of cation local environments and gaining quantitative information of uranium and neptunium valences, a further understanding of neptunium cation incorporation within the orthorhombic structure may be obtained.

AUTHOR INFORMATION

Corresponding Author

*E-mail: renaud.belin@cea.fr.

Notes

The authors declare no competing financial interest.

ACKNOWLEDGMENTS

The authors are grateful to the CEA project CINNA for supporting this work through the postdoctoral funding of M.C.

REFERENCES

(1) Actinide and fission product partitioning and transmutation, Status and assessment report; NEA, OECD, 1999.
(2) Hoekstra, H. R.; Santoro, A.; Siegel, S. *J. Inorg. Nucl. Chem.* **1961**, *18*, 166−178.
(3) Grønvold, F. *J. Inorg. Nucl. Chem.* **1955**, *1*, 357−370.
(4) Blackburn, P. E.; Weissbart, J.; Gulbransen, E. A. *J. Phys. Chem.* **1958**, *62*, 902−908.
(5) Rousseau, G.; Desgranges, L.; Charlot, F.; Millot, N.; Nièpce, J. C.; Pijolat, M.; Valdivieso, F.; Baldinozzi, G.; Bérar, J. F. *J. Nucl. Mater.* **2006**, *355*, 10−20.
(6) Desgranges, L.; Baldinozzi, G.; Rousseau, G.; Niépce, J.-C.; Calvarin, G. *Inorg. Chem.* **2009**, *48*, 7585−592.
(7) Guéneau, C.; Baichi, M.; Labroche, D.; Chatillon, C.; Sundman, B. *J. Nucl. Mater.* **2002**, *304*, 161−175.
(8) Loopstra, B. O. *Acta Crystallogr.* **1970**, *B26*, 656−657.
(9) Garrido, F.; Ibberson, R. M.; Nowicki, L.; Willis, B. T. M. *J. Nucl. Mater.* **2003**, *322*, 87−89.
(10) Richter, K.; Sari, C. *J. Nucl. Mater.* **1987**, *148*, 266−271.
(11) Fahey, J. A.; Turcotte, R. P.; Chikalla, T. D. *J. Inorg. Nucl. Chem.* **1976**, *38*, 495−500.
(12) Paul, R. KFK1297, 1970.
(13) Paul, R.; Keller, C. *J. Nucl. Mater.* **1971**, *41*, 133−142.
(14) Alain, T. FRNC-TH-1146, 1981.
(15) Yamashita, T.; Nitani, N.; Ohuchi, K.; Muromura, T.; Tsuji, T.; Inagaki, H.; Kato, T. *J. Alloys Compd.* **1994**, *213-214*, 375−377.
(16) Finch, R. J.; Kropf, A. *J. MRS Proc.* **2002**, 757.
(17) Markin, T. L.; Street, R. S.; Crouch, E. C. *J. Inorg. Nucl. Chem.* **1970**, *32*, 59−75.
(18) Diehl, H. G.; Keller, C. *J. Solid State Chem.* **1971**, *3*, 621−636.
(19) Beals, R. J.; Handwerk, J. H. *J. Am. Ceram. Soc* **1965**, *48*, 271−274.
(20) Benedict, U.; Dabos, S.; Dufour, C.; Spirlet, J. C.; Pagès, M. *J. Less Common Met.* **1986**, *121*, 461−468.
(21) Benedict, U. *J. Less Common Met.* **1987**, *128*, 7−45.
(22) Markin, T. L.; Street, R. S. *J. Inorg. Nucl. Chem.* **1967**, *29*, 2265−2280.
(23) Tennery, V. J.; Godfrey, T. G. *J. Am. Ceram. Soc.* **1973**, *56*, 129−133.
(24) Dubrovinsky, L. S.; Saxena, S. K. *Phys. Chem. Miner.* **1997**, *24*, 547−550.
(25) *TOPAS V4: General profile and structure analysis software for powder diffraction data. User's manual*; Bruker AXS: Madison, WI, 2005.
(26) Pawley, G. S. *J. Appl. Crystallogr.* **1981**, *14*, 357−361.
(27) Cheary, R. W. *J. Appl. Crystallogr.* **1992**, *25*, 109−121.
(28) Yamashita, T.; Nitani, N.; Tsuji, T.; Inagaki, H. *J. Nucl. Mater.* **1997**, *245*, 72−78.
(29) Benedict, U.; Sari, C. European Atomic Energy Community (Euratom), 1969; 4136 e.
(30) Brett, N. H.; Fox, A. C. *J. Inorg. Nucl. Chem.* **1966**, *28*, 1191−1203.
(31) Benedict, U. *J. Nucl. Mater.* **1970**, *35*, 356−361.
(32) Nawada, H. P.; Sriramamurti, P.; Kutty, K. V. G.; Rajagopalan, S.; Yadav, R. B.; Rao, P. R. V.; Mathews, C. K. *J. Nucl. Mater.* **1986**, *139*, 19−26.